Identification of Differential ER-Alpha Versus ER-Beta Mediated Activation of eNOS in Ovine Uterine Artery Endothelial Cells[1]

Mayra B. Pastore,[3] Saira Talwar,[3] Meghan R. Conley,[3] and Ronald R. Magness[2,3,4,5,6]

[3]Department of Obstetrics & Gynecology Perinatal Research Labs, University of Wisconsin-Madison, Madison, Wisconsin
[4]Department of Animal Sciences, University of Wisconsin-Madison, Madison, Wisconsin
[5]Department of Pediatrics, University of Wisconsin-Madison, Madison, Wisconsin
[6]University of South Florida Perinatal Research Center, Tampa, Florida

ABSTRACT

Endothelial nitric oxide (NO) production is partly responsible for maintenance of uterine vasodilatation during physiologic states of high circulating estrogen levels, e.g., pregnancy. Although 3%–5% of estrogen receptors (ER-alpha/beta) localize to the endothelial plasmalemma, these receptors are responsible for the nongenomic vasodilator responses. Estradiol induces endothelial NO synthase (eNOS) activation to increase NO production; however, it is unknown if eNOS regulation is dependent on both ERs. We hypothesize that ER-alpha and/or ER-beta are capable of changing eNOS phosphorylation and increasing NO production in uterine artery endothelial cells (UAECs). UAECs were 1) treated with vehicle or increasing concentrations (0.1–100 nM) or timed treatments (0–30 min) of estradiol and 2) pretreated with the inhibitors ICI 182,780 (nonspecific ER), 1,3-Bis(4-hydroxyphenyl)-4-methyl-5-[4-(2-piperidinylethoxy)phenol]-1H-pyrazole dihydrochloride (MPP; ER-alpha specific), or 4-[2-phenyl-5,7-bis(trifluoromethyl)pyrazolo[1,5-a]pyrimidin-3-yl]phenol (PHTPP; ER-beta specific) followed by estradiol to analyze the changes in eNOS stimulatory ^{Ser1177}eNOS and ^{Ser635}eNOS versus inhibitory ^{Thr495}eNOS via Western blot analysis. UAECs were also pretreated with MPP, PHTPP, or MPP + PHTTP followed by estradiol or treated with the agonists estradiol, 4,4′,4″-(4-propyl-[1H]-pyrazole-1,3,5-triyl)trisphenol, 2,3-bis(4-hydroxyphenyl)-propionitrile, or ATP to quantify total NOx levels (NO_2+NO_3). Estrogen and ER-alpha activation induced an increase in ^{Ser1177}eNOS and ^{Ser635}eNOS, a decrease in ^{Thr495}eNOS, and an increase in NOx levels. In contrast, ER-beta activation only reduced ^{Thr495}eNOS without changes in ^{Ser1177}eNOS or ^{Ser635}eNOS. However, ER-beta activation increased NOx levels. Lastly, the antagonism of both receptors induced a reduction in basal and stimulated NOx levels in UAECs. These data demonstrate that 1) eNOS phosphorylation changes occur via ER-alpha- and ER-beta-dependent mechanisms and 2) ER-alpha and ER-beta can both increase NO levels independently from each other.

endothelial cells, eNOS, ERα, ERβ, estradiol, estrogen, estrogen receptor, nitric oxide, NO, pregnancy, uterine vasculature

INTRODUCTION

Pregnancy-induced elevations in uterine blood flow (UBF) are temporally associated with concurrent increases in plasma estradiol-17β ($E_2β$) levels [1], which are thought to be partly responsible for increasing the expression and activity of endothelial NO synthase (eNOS) [2–4]. Utilizing ovariectomized animal models, several laboratories have demonstrated a marked increase in UBF after exogenous administration of $E_2β$ [5–7]. Additionally, in vivo studies have established the physiologic cause-effect relationship between systemic administration of $E_2β$ and local inhibition of either estrogen receptors (ERs; with ICI 182,780) or NO synthase (with L-NAME) [8–10]. Furthermore, during pregnancy these specific inhibitors, ICI 182,780 and L-NAME, also partially reduced (25%–30%) uteroplacental blood flow from its maximal levels, thus delineating the relationship of endogenous $E_2β$ and de novo synthesis of NO through eNOS [8, 10, 11]. $E_2β$ is known to induce its estrogenic effects by binding to its two classical receptors, ERα and ERβ [12]. It is clinically important to understand the role of both ERs in the uterine and the placental vasculature because both ERs were shown to induce estrogenic effects in a tissue- and species-specific manner while also differing in their expression patterns in uterine arteries isolated from normal versus severe preeclampsia patients [10, 13–19]. Studies have detailed the $E_2β$-ERα molecular mechanism in the cardiovascular system and to some extent in the uterine vasculature [10, 13–16, 20–22]. However, studies identifying the $E_2β$-ERβ role or the molecular pathways involved in increasing NO bioavailability in the uterine vasculature are still lacking [10, 13–16, 20–22].

Endothelial NO synthase has a complex regulatory mechanism that correctly targets the enzyme to the caveolae and controls the NO bioavailability in the endothelium [13, 23]. It is regulated by protein-protein interactions and posttranslational modifications that can render the enzyme more or less active [13, 23–25]. For example, changes in stimulatory phosphorylation sites ^{Ser1177}eNOS and ^{Ser635}eNOS or the inhibitory phosphorylation site ^{Thr495}eNOS function to tightly control the amount of NO produced by endothelial cells [13, 26–32]. Treatments of endothelial cells with $E_2β$ [14, 33], as well as the calcium-mobilizing agonists such as ATP [25, 31] and bradykinin [34], can induce the posttranslational modifications of eNOS resulting in activation. However, the

comprehensive changes in all of the three key eNOS phosphorylation sites and their overall role in NO production under the exogenous stimulation via ERα and/or ERβ in vitro are still unclear. Therefore, we hypothesize that ERα and/or ERβ will alter eNOS stimulatory and inhibitory phosphorylation sites while also increasing NO production in uterine artery endothelial cells (UAECs). The aims for this study are 1) to establish the time and dose relationship between $E_2\beta$ and changes in eNOS stimulatory phosphorylation sites [Ser1177]eNOS and [Ser635]eNOS and the inhibitory phosphorylation site [Thr495]eNOS and 2) to identify and compare the roles of ERα and ERβ in altering the phosphorylation state of eNOS and NO production.

MATERIALS AND METHODS

The Animal Care and Use Committee of the University of Wisconsin-Madison approved procedures for obtaining uterine arteries from pregnant ewes (UAECs) at Day 120–130; term = 147. The collected uterine arteries were then used for endothelial cell isolation using collagenase digestion procedures [35] and fluorescent-activated cell sorting (FACS) with Alexa 488 acetylated low-density lipoprotein (LDL) (L-23380; Invitrogen).

Cell Culture Preparation

The isolated and validated UAECs were cultured in growth medium HyClone minimal essential medium with Earle with 20% fetal bovine serum (FBS), 100 mg/ml penicillin, and 100 mg/ml streptomycin and propagated [35]. For experiments, passage 3, UAECs were plated in T75 flasks containing phenol-free endothelial basal medium (EBM; Lonza) supplemented with 20% FBS and 1% penicillin-streptomycin. Cells were treated with appropriate drug treatment and lysed for Western blotting and/or the media were collected for NO metabolites ($NO_2 + NO_3$) analysis.

Experimental Treatments and Receptor Blockade

Experiments were performed in at least three different UAEC preparations. For time and concentration-response studies, UAECs grown in six-well plates were serum starved (24 h) in EBM, and the medium was replaced with EBM vehicle (control) or EBM containing $E_2\beta$ (Cat. No. 2824; Tocris) at 0.01, 0.1, 1.0, 10, and 100 nmol/L for 10 min or with EBM containing 10 nmol/L for 0, 5, 10, 15, and 30 min. The 10 nmol/L $E_2\beta$ concentration was chosen based on the concentration-response studies.

The specific agonist treatments were done using 4,4′,4″-(4-propyl-[1H]-pyrazole-1,3,5-triyl)trisphenol (PPT; ERα-specific agonist with ~410-fold binding preference towards ERα over ERβ [12]; Cat. No. 1426; Tocris) at 0.01, 0.1, 1.0, 10, and 100 nmol/L for 20 min and 2,3-bis(4-hydroxyphenyl)-propionitrile (DPN; ERβ-specific agonist with a ~70-fold binding preference towards ERβ over ERα [36]; Cat. No. 1494; Tocris) at 0.01, 0.1, 1.0, 10, and 50 nmol/L for 20 min. Samples were lysed and analyzed with Western immunoblotting.

For analysis of NO metabolites, NO_2 and NO_3 (NO_x), UAECs were treated with vehicle modified Krebs buffer (HEPES 25 mmol/L, NaCl 125 mmol/L, KCl 5 mmol/L, $MgSO_4$ $7H_2O$ 1 mmol/L, KH_2PO_4 1 mmol/L, glucose 6 mmol/L, adjusted to pH = 7.4) or modified Krebs buffer containing $E_2\beta$ at 10 or 100 nmol/L; PPT at 1.0 nmol/L; DPN at 1.0 nmol/L; or ATP at 100 μmol/L for 0, 10, 20, and 30 min.

ER blockades were performed using the nonspecific ER antagonist ICI 182,780 (7α,17β-[9-[(4,4,5,5,5-pentafluoropentyl)sulfinyl]nonyl]estra-1,3,5(10)-triene-3,17-diol; Cat. No. 1047; Tocris) at 100 nmol/L, 1,3-bis(4-hydroxyphenyl)-4-methyl-5-[4-(2-piperidinylethoxy)phenol]-1H-pyrazole dihydrochloride at 100 nmol/L (MPP dihydrochloride; ERα-specific antagonist with a ~200-fold binding preference towards ERα over ERβ [37]; Cat. No. 1991; Tocris), or 4-[2-phenyl-5,7-bis(trifluoromethyl)pyrazolo[1,5-a]pyrimidin-3-yl]phenol at 100 nmol/L (PHTPP; ERβ-specific antagonist with a ~36-fold binding preference towards ERβ over ERα [38]; Cat. No. 2662; Tocris). ERs were blocked by pretreating UAECs with the inhibitor for 30 min.

Protein Extraction and Western Immunoblot Analysis

The total cell extracts were collected using a disposable cell scraper, vortexed, and clarified by centrifugation (13 000 × g, 5 min). The protein content of the samples was measured by a Bio-Rad procedure using bovine serum albumin as the standard. Aliquots of the extracts were frozen at −80°C until Western blot analysis could be performed. Equal amounts of total cell lysates were heated to denatured (95°C, 10 min) in Laemmli buffer, separated on precast 4%–20% SDS-PAGE, and electrically (100 V, 55 min) transferred to polyvinylidene fluoride membranes [20, 39]. Membranes were used to identify [Ser1177]eNOS (1:3000 dilution; product no. 9571; Cell Signaling Technologies), [Ser635]eNOS (1:3000 dilution; product no. 07-56; Upstate), and [Thr495]eNOS (1:3000 dilution; product no. 9475; Cell Signaling Technologies). Total eNOS/NOS III was detected using mouse anti-NOS III (1:2000 dilution; product no. 610297; BD Biosciences) and β-actin (loading control) (1:3000 dilution; product no. 4967; Cell Signaling Technologies). The corresponding secondary antibodies used were anti-mouse immunoglobulin G (IgG) horseradish peroxidase (HRP)-linked Ab (1:3000 dilution; product no. NA931; Amersham), and anti-rabbit IgG HRP-linked Ab (1:3000 dilution; product no. 7074; Amersham).

Nitrite and Nitrate (NO_2 and NO_3) Analysis

NO levels were measured using NOx Analyzer (ENO-30) and Insight autosampler (AS-700) from Eicom Corporation. NOx values were calculated per manufacturer's instructions after subtracting the value of the blank well to remove background peak values.

The UAEC preparations (n = 4) used for agonists and antagonist treatments were plated in six-well plates and serum starved in EBM and media was changed to modified Krebs buffer 30 min prior to treatments.

Statistical Analysis

Data are representative of n = 3 or n = 4 separate experiments and presented as means ± SEM; n = UAECs isolated from different animals. ANOVA followed by post hoc Bonferroni (vs. corresponding control) multiple-comparison test or Student t-test when appropriate was used for statistical analysis. Results were considered significant at $P < 0.05$. Statistical analyses were performed with GraphPad Prism 5.0b software.

RESULTS

Estrogen-Induced Dose-Response and Time-Course Curves Identifying Changes in eNOS Phosphorylation in UAECs

Dose-response curves were designed to identify the estrogen dosage that can both increase stimulatory phosphorylation sites and also decrease the inhibitory site. When compared to control samples, $E_2\beta$ increased stimulatory phosphorylation at sites [Ser1177]eNOS and [Ser635]eNOS starting at the physiological concentration of 0.1 nmol/L (Fig. 1A). [Ser1177]eNOS increased to 6.1-fold at 0.1 nmol/L, 5.3-fold at 1.0 nmol/L, 7.8-fold at 10 nmol/L, and 2.34-fold at 100 nmol/L $E_2\beta$. [Ser635]eNOS also increased 9.8-fold at 0.1 nmol/L, 1.2-fold at 1.0 nmol/L, 2.82-fold at 10 nmol/L, and 6.98-fold at 100 nmol/L $E_2\beta$. In addition, the inhibitory phosphorylation site [Thr495]eNOS significantly decreased to 0.24-fold with 10 nmol/L and 100 nmol/L $E_2\beta$ treatments, with an increase of 4.1-fold with 0.1 and no change observed with 1.0 nmol/L (Fig. 1A). We thus selected 10 nmol/L $E_2\beta$ as the optimal concentration to quantify the change in eNOS phosphorylation pattern from 0 to 30 min (Fig. 1C). We observed an increase in [Ser1177]eNOS starting at 5 min and lasting up to 30 min $E_2\beta$ treatment (2.4-, 4.1-, 1.5-, and 3.8-fold, respectively; Fig. 1C). We also observed an $E_2\beta$-induced increase in [Ser635]eNOS that remained elevated for the same period of time when compared to [Ser1177]eNOS, 5–30 min (4.2-, 4.1-, 4.3-, and 6.4-fold, respectively). The reduction in [Thr495]eNOS phosphorylation reached statistical significance after the 15- and 30-min $E_2\beta$ treatments (0.8- and 0.2-fold).

eNOS Phosphorylation Changes in Response to ERα or ERβ Activation in UAECs

To determine if ERα and ERβ can alter eNOS phosphorylation state, UAECs were treated with $E_2\beta$ (10 nmol/L) or
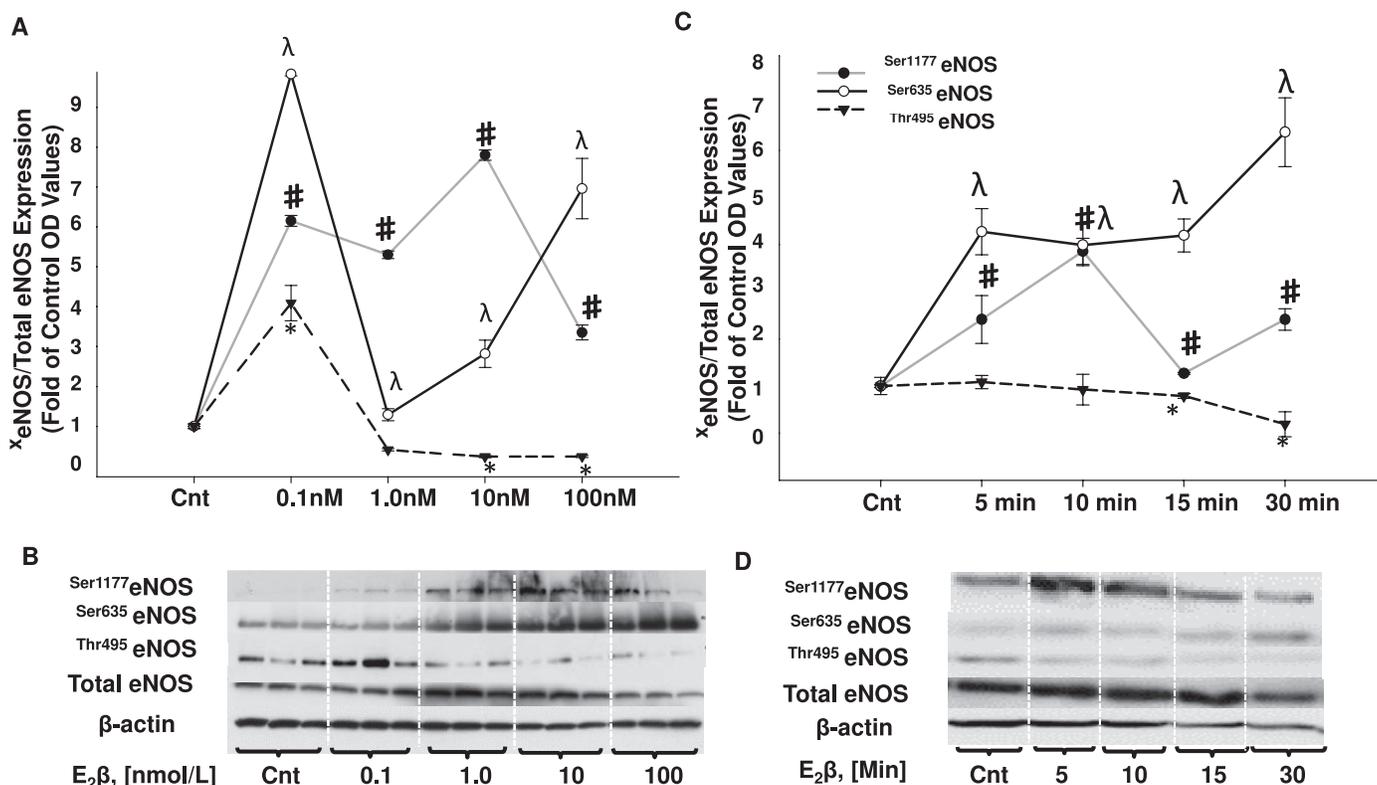
FIG. 1. Estrogen-induced dose responses and time courses for changes in eNOS stimulatory and inhibitory phosphorylation sites in UAECs. **A**) Dose responses: estrogen treatment increased the stimulatory phosphorylation at site ^{Ser1177}eNOS to its highest level of 7.8-fold at 10 nmol/L, and ^{Ser635}eNOS to its highest level of 8.9-fold at 0.1 nmol/L. The inhibitory phosphorylation site ^{Thr495}eNOS was decreased to its lowest level of 0.24-fold at 10 nmol/L and 100 nmol/L $E_2\beta$ treatments. **B**) Representative Western blots for dose-response analysis. **C**) Time-response curves: estrogen treatment increased the stimulatory phosphorylation of ^{Ser1177}eNOS and ^{Ser635}eNOS starting at 5 min and maintained a high level of detection at 30 min treatment. ^{Thr495}eNOS reached a significant reduction at 15 and 30 min estrogen treatment only. **D**) Representative Western blots for time-response analysis. Cnt, control. ^{x}eNOS, phosphorylated eNOS. Symbols denote significance based on phosphorylation site: #, ^{Ser1177}eNOS; λ, ^{Ser635}eNOS; *, ^{Thr495}eNOS; $P < 0.05$.

ERα/β-specific agonists. $E_2\beta$ and PPT (ER-α-specific agonist) similarly increased eNOS stimulatory phosphorylation at sites ^{Ser1177}eNOS and ^{Ser635}eNOS (Fig. 2, A and B). For ^{Ser1177}eNOS, $E_2\beta$ induced a 1.49-fold increase; PPT increased ^{Ser1177}eNOS to 1.12-fold at 0.1 nmol/L, 1.086-fold at 1.0 nmol/L, 0.95-fold at 10 nmol/L, and 1.27-fold at 100 nmol/L. $E_2\beta$ induced a 1.93-fold increase in ^{Ser635}eNOS whereas PPT increased 1.21-fold at 0.1 nmol/L, 1.82-fold at 1.0 nmol/L, 1.4-fold at 10 nmol/L, and 2.0-fold at 100 nmol/L. $E_2\beta$ induced a decrease in the inhibitory phosphorylation at site ^{Thr495}eNOS to 0.71-fold, and PPT decreased phosphorylation at this site to 0.71-fold at 0.1 nmol/L, 0.66-fold at 1.0 nmol/L, 0.64 at 10 nmol/L, and 0.65-fold at 100 nmol/L (Fig. 2C). Dose-response curves for the ERβ-specific agonist DPN were also constructed. We observed the expected $E_2\beta$ increase in ^{Ser1177}eNOS and ^{Ser635}eNOS (1.35-fold and 1.48-fold, respectively; Fig. 3, A and B). However, we observed no change in the stimulatory phosphorylation sites ^{Ser1177}eNOS or ^{Ser635}eNOS (Fig. 3, A and B) under any DPN treatment dose tested. $E_2\beta$ induced a decrease in the inhibitory phosphorylation at site ^{Thr495}eNOS to 0.84-fold. DPN also decreased the inhibitory phosphorylation of ^{Thr495}eNOS to 0.82-fold at 0.1 nmol/L, 0.82-fold at 1.0 nmol/L, 0.84-fold at 10 nmol/L, and 0.85-fold at 50 nmol/L (Fig. 3C).

Effects of Nonspecific ER Inhibitor ICI 182,780 on $E_2\beta$-Induced Changes in eNOS Phosphorylation Sites in UAECs

UAECs were pretreated with ICI 182,780 to determine if ERα and ERβ alter eNOS phosphorylation state. ICI 182,780 alone had no effect on stimulatory phosphorylation sites ^{Ser1177}eNOS and ^{Ser635}eNOS (Fig. 4, A and B), whereas the observed $E_2\beta$-induced increases in ^{Ser1177}eNOS (2.01-fold) and ^{Ser635}eNOS (1.48-fold) were blunted by ICI 182,780 pretreatment (Fig. 4, A and B). The inhibitory phosphorylation at site ^{Thr495}eNOS was removed with $E_2\beta$ treatment (0.86-fold); however, the reduction in ^{Thr495}eNOS was also observed with ICI 182,780 alone (0.93-fold at 0.1 μmol/L, 0.88-fold at 1 μmol/L, and 0.83-fold at 10 μmol/L) or when followed with $E_2\beta$ treatment (0.84-fold at 0.1 μmol/L, 0.85-fold at 1 μmol/L, and 0.81-fold at 10 μmol/L) (Fig. 4C).

Effects of ERα- and ER-β-Mediated Increase in NOx Levels (NO_2 and NO_3) in UAECs

We quantified the total, basal, and stimulated NOx levels ($NO_2 + NO_3$) using an HPLC-based assay by using $E_2\beta$, ERα-specific agonist (PPT), ERβ-specific agonist (DPN), and ATP (positive control) treatments (Fig. 5, A and B). Basal percentage changes of total NOx levels of UAECs were quantified as 16%, 0.7%, and 9% at 10, 20, and 30 min, respectively (Fig. 5A). Concentrations of 10 and 100 nmol/L $E_2\beta$ increased NOx levels by 32% and 62% at 10 min, 64% and 39% at 20 min, and 26% and 20% at 30 min. The 1.0 nmol/L
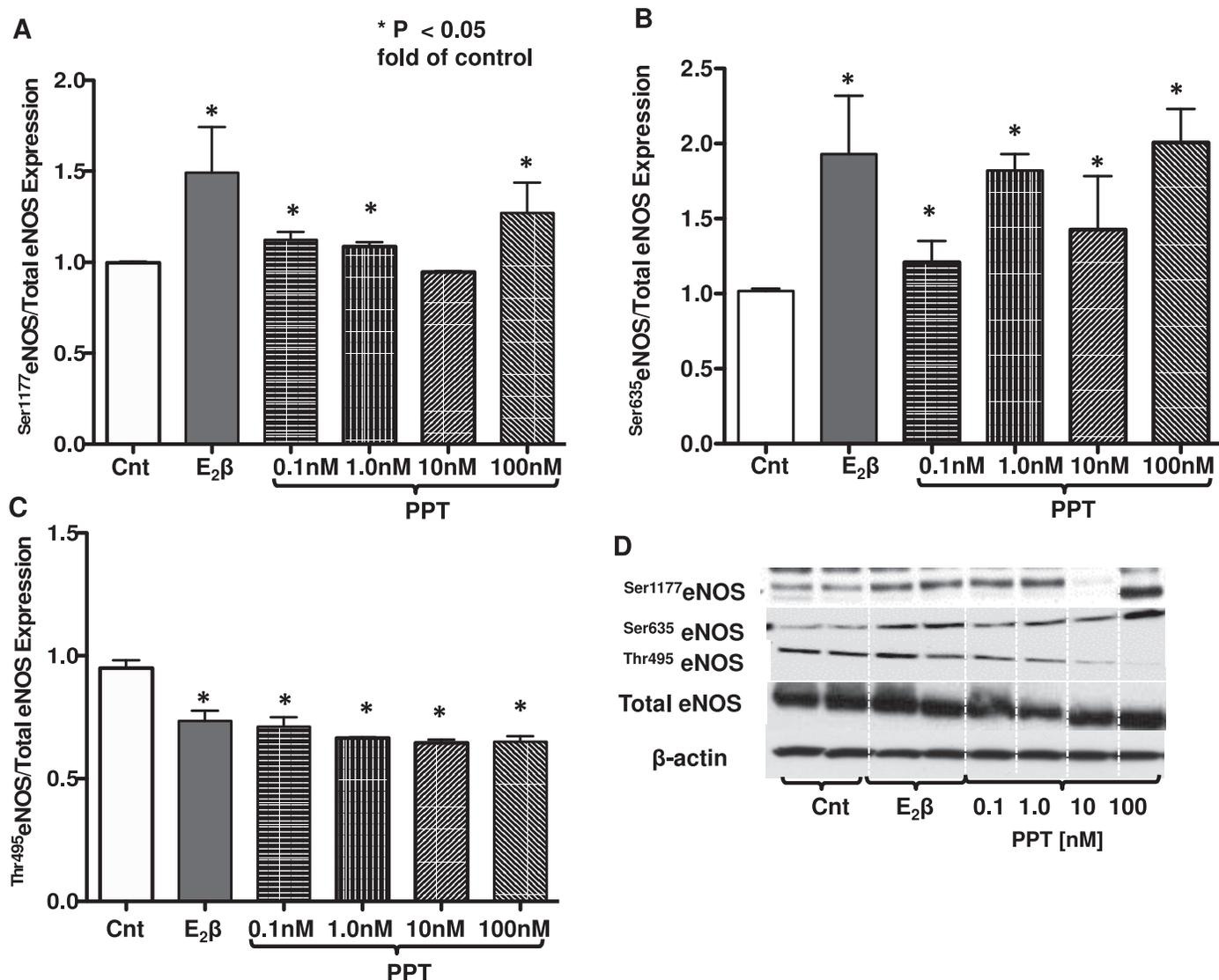
FIG. 2. Changes in eNOS phosphorylation in response to ERα activation in UAECs. **A**) At 20 min, PPT (ERα agonist) increased eNOS stimulatory phosphorylation of ^{Ser1177}eNOS to similar levels as $E_2\beta$. **B**) $E_2\beta$ increased stimulatory phosphorylation of ^{Ser635}eNOS whereas only the highest PPT concentration induced this increase. **C**) $E_2\beta$ and PPT decreased eNOS inhibitory phosphorylation at site ^{Thr495}eNOS. **D**) Representative Western blots for phosphorylated eNOS, total eNOS, and β-actin. Cnt, control. *$P < 0.05$.

PPT and DPN increased NOx levels by 40% and 47% at 10 min, 52% and 34% at 20 min, and 28% and 31% at 30 min. The 100 μmol/L ATP increased NOx levels by 23% at 10 min, 28% at 20 min, and 43% at 30 min.

ICI 182,780 alone did not alter basal NOx levels in UAECs and unexpectedly did not reduce the $E_2\beta$-induced increase in NOx levels (Fig. 5C). Antagonism with 100 nmol/L ERα-specific antagonist (MPP) and ERβ-specific antagonist (PHTPP) were also studied. ERα blockade did not abolish the NOx increase stimulated by the 10 nmol/L $E_2\beta$ treatment (70%) demonstrating residual ERβ actions. The ERβ blockade also did not abolish the NOx increase stimulated by the 10 nmol/L $E_2\beta$ treatment (20%) demonstrating residual ERα actions. However, combining MPP + PHTPP antagonism, we observed the complete abrogation of basal (−16%) and $E_2\beta$-induced increase in NOx levels (−54%) (Fig. 5C), demonstrating that both receptors must be blocked in order to observe a significant reduction in basal and stimulated NOx levels. Finally, these data also validate those observation obtained from ERα/ERβ-specific agonists shown in Figure 5B, where

both receptors were capable of increasing NOx levels when activated.

DISCUSSION

The first aim for this study was to establish the relationship between dose/time and the $E_2\beta$-induced changes in eNOS phosphorylation. The findings herein demonstrated that $E_2\beta$ induced changes in the three key phosphorylation sites of eNOS, indicating that eNOS was rendered more active, i.e., there were higher detected levels of ^{Ser1177}eNOS and ^{Ser635}eNOS and lower detected levels of ^{Thr495}eNOS. The second aim for this study was to identify and compare the roles of ERα and ERβ in altering the phosphorylation state of eNOS and NO production. We presented data that identified for the first time in UAECs that $E_2\beta$-induced changes in eNOS phosphorylation patterns were also observed when ERα or ERβ was activated, albeit not completely equal to the effects observed with $E_2\beta$. Additionally, we observed the impact on
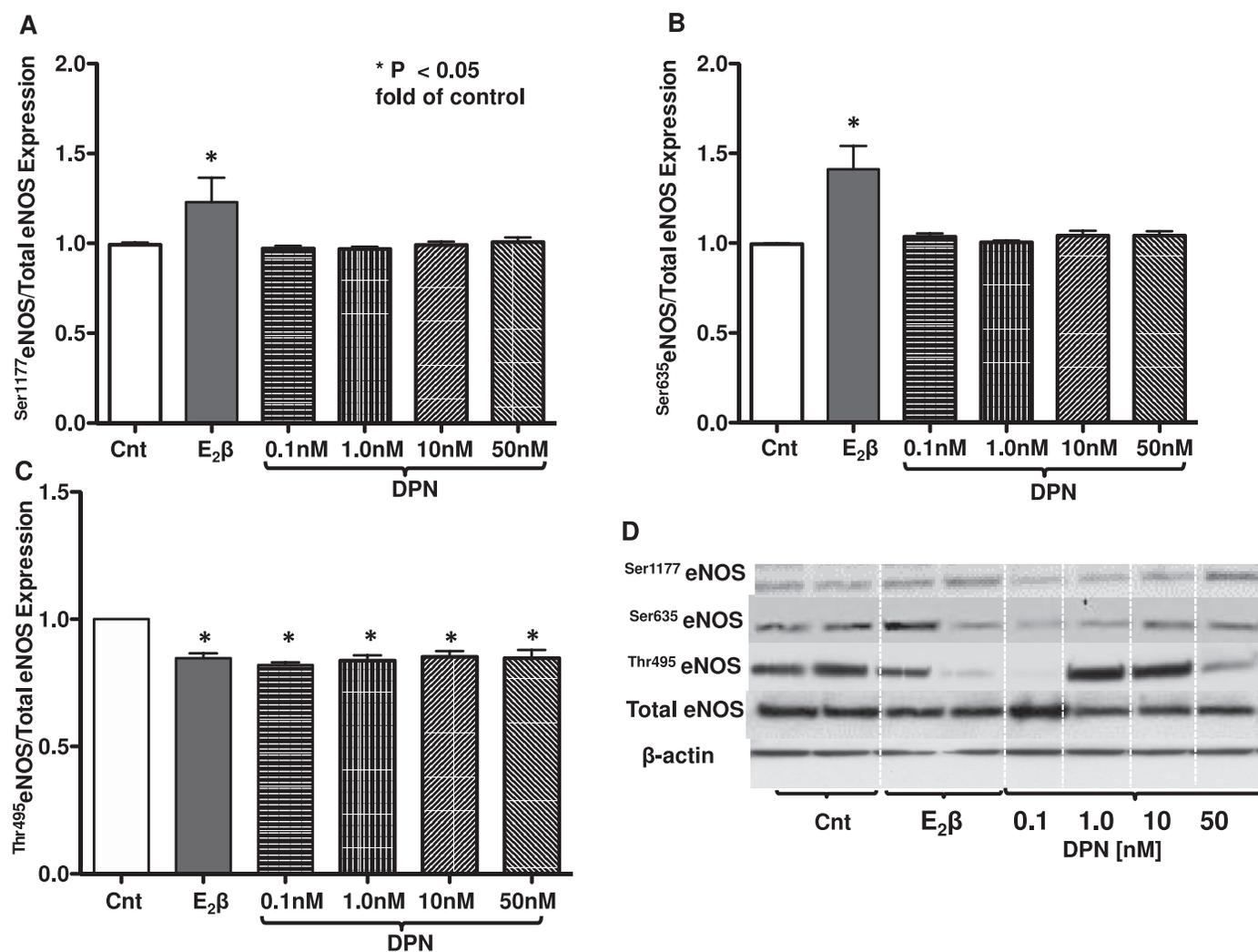
FIG. 3. Changes in eNOS phosphorylation in response to ERβ activation in UAECs. **A**) At 20 min, $E_2\beta$ increased ^{Ser1177}eNOS stimulatory phosphorylation by 1.35-fold whereas DPN had no effect on this site. **B**) $E_2\beta$ increased ^{Ser635}eNOS stimulatory phosphorylation by 1.48-fold whereas DPN did not increase phosphorylation at this site. **C**) $E_2\beta$ induced a decrease in the inhibitory phosphorylation at site ^{Thr495}eNOS by 0.84-fold. DPN also decreased the inhibitory phosphorylation of ^{Thr495}eNOS to 0.82-fold at 0.1 nmol/L, 0.82-fold at 1.0 nmol/L, 0.84-fold at 10 nmol/L, and 0.85-fold at 50 nmol/L. **D**) Representative Western blots for phosphorylated eNOS, total eNOS, and β-actin. Cnt, control. *$P < 0.05$.

basal NOx levels only when both receptors were blocked with their specific agonists.

In UAECs, we have previously identified that $E_2\beta$ and $E_2\beta$-bovine serum albumin conjugate induces an overall increase in eNOS phosphorylation and an increase in the total NOx production, suggesting a role for membrane ERs [14]. However, it was not until this current study that we were able to test the roles for each ER in altering eNOS phosphorylation patterns and the increase in NOx levels in UAECs. Herein, we identified that $E_2\beta$ can alter three key eNOS phosphorylation sites (Fig. 1), rendering the enzyme more active, thus increasing NOx levels (Fig. 5). The activation of ERα (via PPT) increased ^{Ser1177}eNOS and ^{Ser635}eNOS while also decreasing ^{Thr495}eNOS when using 1 nmol/L PPT, a concentration close to its half-maximal response and shown to have ~410-fold preference for ERα over ERβ [12]. The activation of ERβ (via DPN) showed no change in either ^{Ser1177}eNOS or ^{Ser635}eNOS, but decreased the inhibitory phosphorylation at site ^{Thr495}eNOS. The observed change in ^{Thr495}eNOS occurred with all DPN concentrations tested; 50 nmol/L is close to its

half-maximal response and shown to have ~70-fold preference for ERβ over ERα [36]. These observations identified the differences in eNOS posttranslational regulation that occur under the activation of each receptor. Additionally, it is noteworthy that ^{Ser635}eNOS is largely influential over the sustained NO production in UAECs (>30 min) versus the immediate short-term increase in ^{Ser1177}eNOS [25, 40] and was also reported to be decreased when protein kinase A (PKA) [40] or mitogen-activated protein kinase kinase (MEK) [13] pathways were blocked. Moreover, we observed the decrease in ^{Thr495}eNOS with the activation of either ER. Surprisingly, we also observed a decrease in ^{Thr495}eNOS with ICI 182,780, which may point to an additional ER or ER regulatory protein in UAECs yet to be explored in the uterine vasculature. In this regard, GPER-1 is a seven-transmembrane-spanning G-protein-coupled receptor that is activated by ICI 182,780 [41]. Several investigators have shown that GPER-1 can induce rapid estrogenic effects in ERα-positive cancer cells, human endothelial cells, and B-lymphocytes, and it has been implicated in having physiological functions in reproductive

5
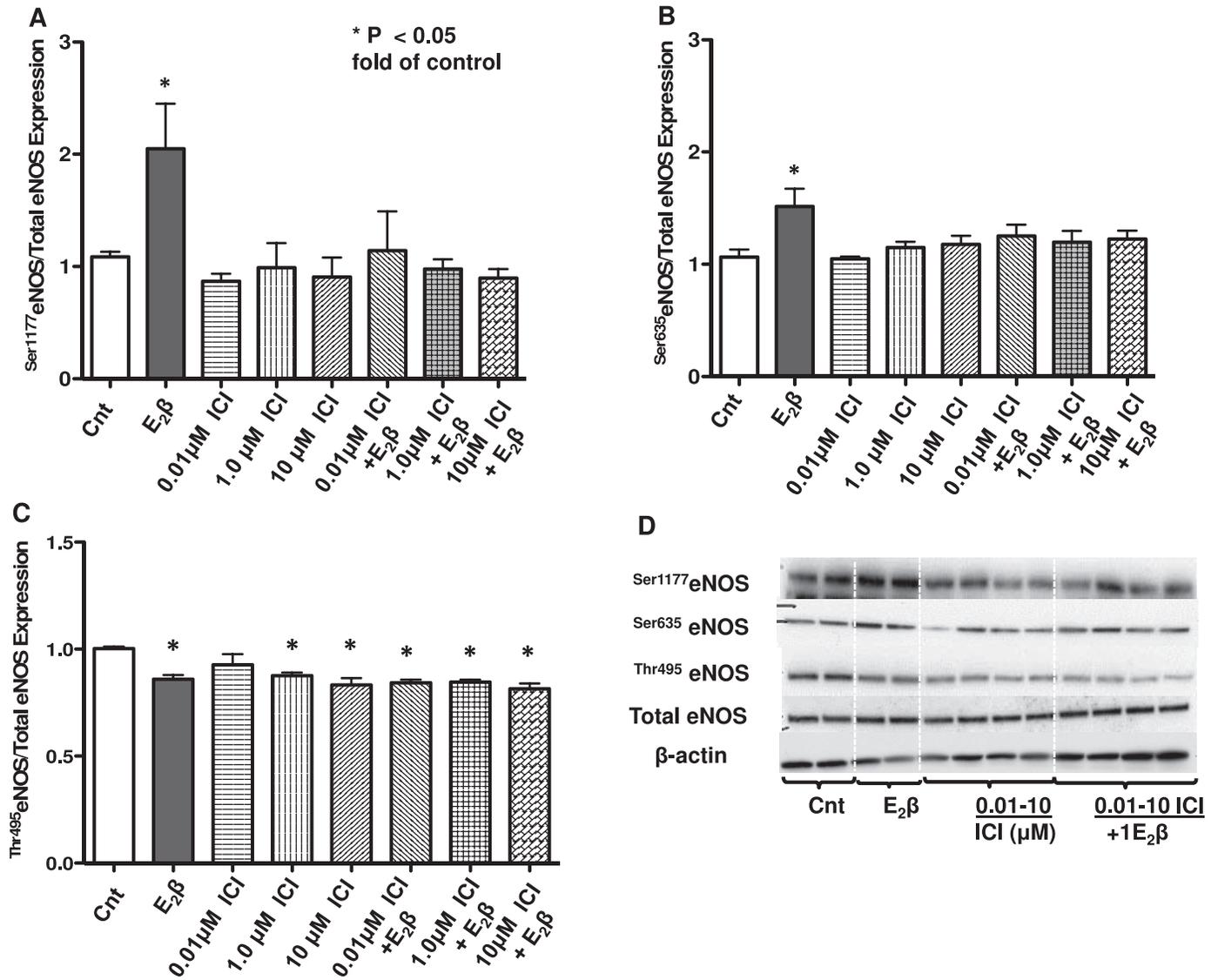
FIG. 4. Effects of nonspecific ER inhibitor ICI 182,780 on $E_2\beta$-induced eNOS phosphorylation changes in UAECs. **A**) $E_2\beta$ increased stimulatory phosphorylation of ^{Ser1177}eNOS, which was blocked by ICI 182,780. **B**) $E_2\beta$ increased stimulatory phosphorylation of ^{Ser635}eNOS, which was also blocked by ICI 182,780. ICI 182,780 alone had no effect on these stimulatory sites. **C**) $E_2\beta$ and ICI 182,780 with or without $E_2\beta$ treatment both decreased inhibitory phosphorylation at site ^{Thr495}eNOS. **D**) Representative Western blots for phosphorylated eNOS, total eNOS, and β-actin. Cnt, control. *$P < 0.05$.

and cardiovascular systems [41, 42]. However, GPER-1 expression or cellular location is unknown in UAECs. But it is important to note that ^{Thr495}eNOS is a key regulatory site because of its location within the Ca^{2+}/calmodulin-binding domain of eNOS; thus, the removal of this phospho group facilitates eNOS binding to Ca^{2+}/calmodulin after an increase of intracellular Ca^{2+} and increasing enzymatic activity and NO bioavailability [13, 40].

The changes in eNOS phosphorylation patterns also validate the functional increase in NOx levels observed under PPT and, to some extent, DPN stimulation observed during our current study of UAECs (Fig. 5B). Our reported increase in NOx levels is in agreement with the relaxation studies conducted in human uterine, placental [19], and rat pulmonary artery [43] studies that also tested vasodilation with ER-specific agonists (PPT and DPN). However, our results differed from aortic artery studies of mice containing a whole-body $ER\alpha$ or $ER\beta$ knockout (KO) phenotype [44]. Darblade et al. identified $ER\alpha$ to be the sole ER responsible for acute vasodilatory effects in mouse

thoracic aortas isolated from $ER\alpha^{-/-}$ or $ER\beta^{-/-}$ KO versus wild-type mice [44]. The effects of a global receptor KO versus the tissue-specific KO responses may explain the difference observed between these studies. Additionally, the circulating estrogens of female versus male subjects can also influence the ER protein levels in a tissue-specific manner, which, in turn, can influence vasodilatory responses via a specific ER [7, 23]. Lastly, our published work highlights the effects of the circulating estrogen levels over the expression pattern of the ERs in reproductive versus nonreproductive vasculature observed during the ovarian cycle and pregnancy [5, 23, 45]. $ER\alpha$ maintained the same level of expression in almost all the vasculatures tested and isolated from animals in the ovarian cycle or pregnant state [23]. In contrast, $ER\beta$ expression levels increased significantly in all the reproductive vasculature isolated from pregnant animals, suggesting a pregnancy-specific adaptation [23]. In addition to changes in ER expression levels, other pregnancy-specific adaptations are observed in freshly isolated UAECs and include increases in
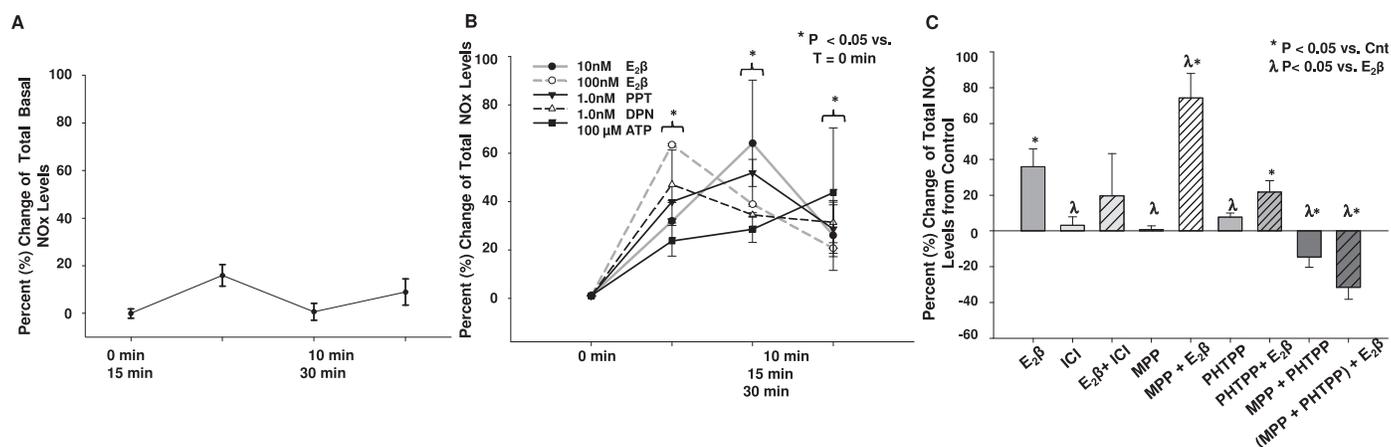
FIG. 5. Effects of ERα and ERβ agonists and antagonists on increases of total percentage change NOx levels (NO_2 and NO_3) in UAECs. Total NOx levels were quantified by the use of an HPLC-based assay. **A)** Basal percentage changes of NOx levels were 16%, 0.7%, and 9% at 10, 20, and 30 min, respectively. **B)** Elevations in UAECs NOx levels were observed with $E_2β$ (10 and 100 nmol/L), PPT, ERα-specific agonist (1 nmol/L), DPN, ERβ-specific agonist (1 nmol/L), and ATP (100 nmol/L) across the 30-min time course. The basal NOx level was set to 0% to quantify the agonist-induced changes. **C)** UAECs were pretreated for 1 h with ICI 182,780 (ICI; 100 nmol/L); MPP, ERα-specific antagonist (100 nmol/L); PHTPP, ERβ-specific antagonist (100 nmol/L); or the combination of MPP + PHTPP (100 nmol/L +100 nmol/L), followed by $E_2β$ treatment (10 nmol/L for 20 min). $E_2β$ increased total NOx levels (65%) above control levels whereas ICI 182,780, MPP, or PHTPP alone had no effect. ICI 182,780 did not reduce the $E_2β$-induced increases in NOx levels. The antagonism of both ERs with MPP + PHTPP showed a decrease of basal NOx levels of −16%. $E_2β$ treatment following MPP + PHTPP antagonists induced further decreases in NOx levels (−54%). $λP < 0.05$ vs. Cnt; $*P < 0.05$ vs. $E_2β$.

eNOS expression, sustained Ca^{2+} signaling, and NO production [46]. We also reported enhanced UAEC proliferation orchestrated via $E_2β/ERβ$ mechanisms; proliferation was used as a marker for physiological uterine angiogenesis necessary during pregnancy [20].

The current study demonstrated the increase in NO levels under $E_2β$ in an ER-specific manner. The blockade studies using MPP or PHTPP (ERα- and ER-β-specific antagonist, respectively) identified that when ERα or ERβ are blocked, the increase in NOx levels observed with $E_2β$ treatment was not blunted; on the contrary, the blockade of ERα showed NOx levels that were greater than $E_2β$ alone, which binds to both ERα and ERβ (Fig. 5B). The mechanisms required for ERα and ERβ for translocation to the plasma membrane have been extensively studied [47]. However, the exact location of ERα and ERβ at the plasma membrane is not completely understood. Plasma membrane fractionation studies published by Chambliss and Shaul have identified ERα within the specialized signaling domains of the plasma membrane called caveolae microdomains [33, 48]. ERα localizes within the caveolae ''signalsomes complexes'' along with Cav-1 and eNOS to facilitate the signaling mechanism for rapid and controlled NO production [33, 48]. The location of ERβ at the plasma membrane and/or within the caveolae is a topic that requires further study; however, it is also possible that differences in ER location may provide an unappreciated alternative signaling mechanism for endogenous ERβ to activate eNOS in UAECs. The alternative signaling mechanism may explain the increased level of total NOx observed after the blockade of ERα in our studies (Fig. 5B). Alternatively, differences in NOx levels observed during this study may also point to pregnancy-specific adaptations in the redundant signaling machinery documented in UAECs, which affect the complex eNOS regulation [13, 20, 35].

Basal NO levels are important in the homeostatic maintenance of the systemic and uterine vascular tone. Several investigators have shown, using animal models, that the decrease in basal NO bioavailability is involved in the development of hypertension [49, 50]. Our data show that when both ERs are blocked with their specific antagonists

(MPP + PHTPP) there is a reduction in total basal NOx levels to lower levels than those of controls (Fig. 5C). These results are in line with studies that analyzed the effects on vasodilation, both the basal and stimulated NO production, in mouse aorta rings [51] and the endothelial-dependent relaxation of the forearm from offspring of parents with essential hypertension [52]. However, the present study is the first to show that the concurrent blockade of endogenous ERα and ERβ can lead to diminished basal NOx levels, which are further exacerbated by estrogen treatment (Fig. 5C). Thus, we observed a link between ER dysregulation and the basal NOx levels in UAECs (Fig. 5A). However, the paradigm that estrogen treatment further decreases NOx levels may be explained by the dysregulation of ERs leading to altered eNOS posttranslational modifications, protein-protein interactions, and/or intracellular Ca^{2+} that are required for the enzyme's activity in UAECs [13, 14]. The basal NO regulation may point to a critical step in vasodilatory dysfunction observed in pregnancy-related hypertensive disorders given that estrogens and estrogen metabolite synthesis become aberrant in patients with severe preeclampsia [53] and ER levels change during the ovarian cycle and pregnancy [39].

In summary, the present study demonstrates that estrogen via the activation of both ERs (ERα/ERβ) induced an increase in eNOS stimulatory phosphorylation sites [Ser1177]eNOS and [Ser635]eNOS, a decrease in the inhibitory phosphorylation site [Thr495]eNOS, and an increase in total NOx levels in UAECs. We also provide evidence that the activation of ERα mirrors the eNOS phosphorylation pattern observed with estrogen and increased total NOx levels. In contrast, ERβ activation only induced a reduction in the inhibitory phosphorylation site, [Thr495]eNOS, but ERβ activation still induced an increase in total NOx levels, thus identifying an important regulatory site for eNOS in UAECs. These data demonstrate that activation of either ERα or ERβ leads to the increase in NO bioavailability. Lastly, another important finding from this study is the observed dysregulation of basal NOx levels that occurs only when ERα and ERβ are concurrently antagonized with their respective inhibitors. Basal NO levels are an important mechanism for vascular tone. Therefore, future studies may

need to test the basal dysregulation we observed in vitro in an ex vivo and/or in vivo setting and whether this dysregulation is involved in the progression of hypertensive disorders such as preeclampsia.

ACKNOWLEDGMENT

REFERENCES

1. Killam AP, Rosenfeld CR, Battaglia FC, Makowski EL, Meschia G. Effect of estrogens on the uterine blood flow of oophorectomized ewes. Am J Obstet Gynecol 1973; 115:1045–1052.

2. Magness RR, Rosenfeld CR. Local and systemic estradiol-17 beta: effects on uterine and systemic vasodilation. Am J Physiol 1989; 256: E536–E542.

3. Vagnoni KE, Shaw CE, Phernetton TM, Meglin BM, Bird IM, Magness RR. Endothelial vasodilator production by uterine and systemic arteries. III. Ovarian and estrogen effects on NO synthase. Am J Physiol 1998; 275: H1845–H1856.

4. Magness RR, Shaw CE, Phernetton TM, Zheng J, Bird IM. Endothelial vasodilator production by uterine and systemic arteries. II. Pregnancy effects on NO synthase expression. Am J Physiol 1997; 272: H1730–H1740.

5. Magness RR, Parker CR Jr, Rosenfeld CR. Systemic and uterine responses to chronic infusion of estradiol-17 beta. Am J Physiol 1993; 265: E690–E698.

6. Rosenfeld CR, Roy T, Cox BE. Mechanisms modulating estrogen-induced uterine vasodilation. Vascul Pharmacol 2002; 38:115–125.

7. Sladek SM, Magness RR, Conrad KP. Nitric oxide and pregnancy. Am J Physiol 1997; 272:R441–R463.

8. Magness RR, Rosenfeld CR, Hassan A, Shaul PW. Endothelial vasodilator production by uterine and systemic arteries. I. Effects of ANG II on PGI2 and NO in pregnancy. Am J Physiol 1996; 270:H1914–H1923.

9. Rosenfeld CR, Cox BE, Roy T, Magness RR. Nitric oxide contributes to estrogen-induced vasodilation of the ovine uterine circulation. J Clin Invest 1996; 98:2158–2166.

10. Magness RR, Phernetton TM, Gibson TC, Chen DB. Uterine blood flow responses to ICI 182 780 in ovariectomized oestradiol-17beta-treated, intact follicular and pregnant sheep. J Physiol 2005; 565:71–83.

11. Miller SL, Jenkin G, Walker DW. Effect of nitric oxide synthase inhibition on the uterine vasculature of the late-pregnant ewe. Am J Obstet Gynecol 1999; 180:1138–1145.

12. Kraichely DM, Sun J, Katzenellenbogen JA, Katzenellenbogen BS. Conformational changes and coactivator recruitment by novel ligands for estrogen receptor-alpha and estrogen receptor-beta: correlations with biological character and distinct differences among SRC coactivator family members. Endocrinology 2000; 141:3534–3545.

13. Ramadoss J, Pastore MB, Magness RR. Endothelial caveolar subcellular domain regulation of endothelial nitric oxide synthase. Clin Exp Pharmacol Physiol 2013; 40:753–764.

14. Chen DB, Bird IM, Zheng J, Magness RR. Membrane estrogen receptor-dependent extracellular signal-regulated kinase pathway mediates acute activation of endothelial nitric oxide synthase by estrogen in uterine artery endothelial cells. Endocrinology 2004; 145:113–125.

15. Monje P, Zanello S, Holick M, Boland R. Differential cellular localization of estrogen receptor alpha in uterine and mammary cells. Mol Cell Endocrinol 2001; 181:117–129.

16. Cruz MN, Douglas G, Gustafsson JA, Poston L, Kublickiene K. Dilatory responses to estrogenic compounds in small femoral arteries of male and female estrogen receptor-beta knockout mice. Am J Physiol Heart Circ Physiol 2006; 290:H823–H829.

17. Muller-Delp JM, Lubahn DB, Nichol KE, Philips BJ, Price EM, Curran EM, Laughlin MH. Regulation of nitric oxide-dependent vasodilation in coronary arteries of estrogen receptor-alpha-deficient mice. Am J Physiol Heart Circ Physiol 2003; 285:H2150–H2157.

18. Yin G, Zhu X, Guo C, Yang Y, Han T, Chen L, Yin W, Gao P, Zhang H, Geng J, Wang J, Liang L. Differential expression of estradiol and estrogen receptor alpha in severe preeclamptic pregnancies compared with normal pregnancies. Mol Med Report 2013; 7:981–985.

19. Corcoran JJ, Nicholson C, Sweeney M, Charnock JC, Robson SC, Westwood M, Taggart MJ. Human uterine and placental arteries exhibit tissue-specific acute responses to 17beta-estradiol and estrogen-receptor-specific agonists. Mol Hum Reprod 2014; 20:433–441.

20. Jobe SO, Ramadoss J, Koch JM, Jiang Y, Zheng J, Magness RR. Estradiol-17beta and its cytochrome P450- and catechol-O-methyltransferase-derived metabolites stimulate proliferation in uterine artery endothelial cells: role of estrogen receptor-alpha versus estrogen receptor-beta. Hypertension 2010; 55:1005–1011.

21. Chen Z, Yuhanna IS, Galcheva-Gargova Z, Karas RH, Mendelsohn ME, Shaul PW. Estrogen receptor alpha mediates the nongenomic activation of endothelial nitric oxide synthase by estrogen. J Clin Invest 1999; 103: 401–406.

22. Simoncini T, Hafezi-Moghadam A, Brazil DP, Ley K, Chin WW, Liao JK. Interaction of oestrogen receptor with the regulatory subunit of phosphatidylinositol-3-OH kinase. Nature 2000; 407:538–541.

23. Pastore MB, Jobe SO, Ramadoss J, Magness RR. Estrogen receptor-alpha and estrogen receptor-beta in the uterine vascular endothelium during pregnancy: functional implications for regulating uterine blood flow. Semin Reprod Med 2012; 30:46–61.

24. Haynes MP, Sinha D, Russell KS, Collinge M, Fulton D, Morales-Ruiz M, Sessa WC, Bender JR. Membrane estrogen receptor engagement activates endothelial nitric oxide synthase via the PI3-kinase-Akt pathway in human endothelial cells. Circ Res 2000; 87:677–682.

25. Mount PF, Kemp BE, Power DA. Regulation of endothelial and myocardial NO synthesis by multi-site eNOS phosphorylation. J Mol Cell Cardiol 2007; 42:271–279.

26. Gratton JP, Fontana J, O'Connor DS, Garcia-Cardena G, McCabe TJ, Sessa WC. Reconstitution of an endothelial nitric-oxide synthase (eNOS), hsp90, and caveolin-1 complex in vitro. Evidence that hsp90 facilitates calmodulin stimulated displacement of eNOS from caveolin-1. J Biol Chem 2000; 275:22268–22272.

27. Harris MB, Ju H, Venema VJ, Blackstone M, Venema RC. Role of heat shock protein 90 in bradykinin-stimulated endothelial nitric oxide release. Gen Pharmacol 2000; 35:165–170.

28. Ramadoss J, Liao WX, Morschauser TJ, Lopez GE, Patankar MS, Chen DB, Magness RR. Endothelial caveolar hub regulation of adenosine triphosphate-induced endothelial nitric oxide synthase subcellular partitioning and domain-specific phosphorylation. Hypertension 2012; 59: 1052–1059.

29. Venema RC. Post-translational mechanisms of endothelial nitric oxide synthase regulation by bradykinin. Int Immunopharmacol 2002; 2: 1755–1762.

30. Fleming I, Busse R. Signal transduction of eNOS activation. Cardiovasc Res 1999; 43:532–541.

31. Yi F, Boeldt DS, Magness RR, Bird IM. [Ca2+]i signaling vs eNOS expression as determinants of NO output in uterine artery endothelium: relative roles in pregnancy adaptation and reversal by VEGF165. Am J Physiol Heart Circ Physiol 2011; 300:H1182–H1193.

32. Boo YC, Sorescu G, Boyd N, Shiojima I, Walsh K, Du J, Jo H. Shear stress stimulates phosphorylation of endothelial nitric-oxide synthase at Ser1179 by Akt-independent mechanisms: role of protein kinase A. J Biol Chem 2002; 277:3388–3396.

33. Chambliss KL, Yuhanna IS, Mineo C, Liu P, German Z, Sherman TS, Mendelsohn ME, Anderson RG, Shaul PW. Estrogen receptor alpha and endothelial nitric oxide synthase are organized into a functional signaling module in caveolae. Circ Res 2000; 87:E44–E52.

34. Bernier SG, Haldar S, Michel T. Bradykinin-regulated interactions of the mitogen-activated protein kinase pathway with the endothelial nitric-oxide synthase. J Biol Chem 2000; 275:30707–30715.

35. Bird IM, Sullivan JA, Di T, Cale JM, Zhang L, Zheng J, Magness RR. Pregnancy-dependent changes in cell signaling underlie changes in differential control of vasodilator production in uterine artery endothelial cells. Endocrinology 2000; 141:1107–1117.

36. Meyers MJ, Sun J, Carlson KE, Marriner GA, Katzenellenbogen BS, Katzenellenbogen JA. Estrogen receptor-beta potency-selective ligands: structure-activity relationship studies of diarylpropionitriles and their acetylene and polar analogues. J Med Chem 2001; 44:4230–4251.

37. Sun J, Meyers MJ, Fink BE, Rajendran R, Katzenellenbogen JA, Katzenellenbogen BS. Novel ligands that function as selective estrogens or antiestrogens for estrogen receptor-alpha or estrogen receptor-beta. Endocrinology 1999; 140:800–804.

38. Compton DR, Sheng S, Carlson KE, Rebacz NA, Lee IY, Katzenellenbogen BS, Katzenellenbogen JA. Pyrazolo[1,5-a]pyrimidines: estrogen receptor ligands possessing estrogen receptor beta antagonist activity. J Med Chem 2004; 47:5872–5893.

39. Liao WX, Magness RR, Chen DB. Expression of estrogen receptors-alpha and -beta in the pregnant ovine uterine artery endothelial cells in vivo and in vitro. Biol Reprod 2005; 72:530–537.

40. Boo YC, Hwang J, Sykes M, Michell BJ, Kemp BE, Lum H, Jo H. Shear stress stimulates phosphorylation of eNOS at Ser(635) by a protein kinase A-dependent mechanism. Am J Physiol Heart Circ Physiol 2002; 283: H1819–H1828.

41. Meyer MR, Prossnitz ER, Barton M. GPER/GPR30 and regulation of vascular tone and blood pressure. Immunol Endocr Metab Agents Med Chem 2011; 11:255–261.

42. Prossnitz ER, Barton M. Estrogen biology: new insights into GPER function and clinical opportunities. Mol Cell Endocrinol 2014; 389:71–83.

43. Lahm T, Crisostomo PR, Markel TA, Wang M, Wang Y, Tan J, Meldrum DR. Selective estrogen receptor-alpha and estrogen receptor-beta agonists rapidly decrease pulmonary artery vasoconstriction by a nitric oxide-dependent mechanism. Am J Physiol Regul Integr Comp Physiol 2008; 295:R1486–R1493.

44. Darblade B, Pendaries C, Krust A, Dupont S, Fouque MJ, Rami J, Chambon P, Bayard F, Arnal JF. Estradiol alters nitric oxide production in the mouse aorta through the alpha-, but not beta-, estrogen receptor. Circ Res 2002; 90:413–419.

45. Gifford SM, Cale JM, Tsoi S, Magness RR, Bird IM. Pregnancy-specific changes in uterine artery endothelial cell signaling in vivo are both programmed and retained in primary culture. Endocrinology 2003; 144: 3639–3650.

46. Yi FX, Magness RR, Bird IM. Simultaneous imaging of [Ca2+]i and intracellular NO production in freshly isolated uterine artery endothelial cells: effects of ovarian cycle and pregnancy. Am J Physiol Regul Integr Comp Physiol 2005; 288:R140–R148.

47. Acconcia F, Ascenzi P, Bocedi A, Spisni E, Tomasi V, Trentalance A, Visca P, Marino M. Palmitoylation-dependent estrogen receptor alpha membrane localization: regulation by 17beta-estradiol. Mol Biol Cell 2005; 16:231–237.

48. Chambliss KL, Shaul PW. Rapid activation of endothelial NO synthase by estrogen: evidence for a steroid receptor fast-action complex (SRFC) in caveolae. Steroids 2002; 67:413–419.

49. Baylis C, Mitruka B, Deng A. Chronic blockade of nitric oxide synthesis in the rat produces systemic hypertension and glomerular damage. J Clin Invest 1992; 90:278–281.

50. Cosentino F, Luscher TF. Maintenance of vascular integrity: role of nitric oxide and other bradykinin mediators. Eur Heart J 1995; 16(suppl K): 4–12.

51. Rubanyi GM, Freay AD, Kauser K, Sukovich D, Burton G, Lubahn DB, Couse JF, Curtis SW, Korach KS. Vascular estrogen receptors and endothelium-derived nitric oxide production in the mouse aorta. Gender difference and effect of estrogen receptor gene disruption. J Clin Invest 1997; 99:2429–2437.

52. McAllister AS, Atkinson AB, Johnston GD, Hadden DR, Bell PM, McCance DR. Basal nitric oxide production is impaired in offspring of patients with essential hypertension. Clin Sci 1999; 97:141–147.

53. Jobe SO, Tyler CT, Magness RR. Aberrant synthesis, metabolism, and plasma accumulation of circulating estrogens and estrogen metabolites in preeclampsia implications for vascular dysfunction. Hypertension 2013; 61:480–487.